Moments via Integral Transform Method for 2-D Dielectric Materials

Jerry R. Smith, Jr. and Mark S. Mirotznik

***Abstract*—This paper extends the moments via integral transform method (MITM) which analytically reduces the general method of moments (MoM) impedance equation from a double integral to a single integral thereby significantly reducing the matrix fill time. The MITM makes use of a specialized integral representation of the two dimensional Green's function (Hankel function) and represents the MoM impedance as a single integral in terms of integral transforms which are analytic for nearly arbitrary shape and weight functions.**

***Index Terms*—Electromagnetic scattering, method of moments (MoM), transforms.**

I. Introduction

The fill time of the impedance matrix represents a significant chokepoint in method of moments (MoM) calculations because the matrix elements are expressed as multidimensional integrals. Previous techniques to reduce matrix fill times employed spectral domain representations of the Green's function. Recently, Smith and Mirotznik [1] developed an alternative approach that analytically reduces the two-dimensional (2-D) MoM impedance equation for perfectly electrically conducting (PEC) bodies to a single integral for nearly arbitrary shape and weight functions. This moments via integral transform method (MITM) reduced the fill time of the MoM impedance matrix by over an order of magnitude for some cases. In this paper, we extend the 2-D MITM to general dielectric bodies.

II. MoM

The governing scattering integral equation for a 2-D scatterer C of linear material (ε_1, μ_1) in free space is given by [2, p. 156, eqs. 3.117 and 3.118 and p. 161, eqs. 3.137 and 3.138.][1]

$$F_z^{\rm inc}(\boldsymbol{\rho}) = \int_C \left\{\vartheta_0 B^n(\boldsymbol{\rho}')G_0(\boldsymbol{\rho},\boldsymbol{\rho}') - B^t(\boldsymbol{\rho}')\partial_{n'}G_0(\boldsymbol{\rho},\boldsymbol{\rho}')\right\} \times dC' + \frac{B^t(\boldsymbol{\rho})}{2} \tag{1a}$$

$$0 = \int_C \left\{\vartheta_1 B^n(\boldsymbol{\rho}')G_1(\boldsymbol{\rho},\boldsymbol{\rho}') - B^t(\boldsymbol{\rho}')\partial_{n'}G_1(\boldsymbol{\rho},\boldsymbol{\rho}')\right\} \times dC' - \frac{B^t(\boldsymbol{\rho})}{2} \tag{1b}$$

where $\boldsymbol{\rho} \in C$, the Green's function [2, p. 18, eq. 1.117][2] is $G_j(\boldsymbol{\rho},\boldsymbol{\rho}') \equiv (1/4i)H_0^{(1)}(\kappa_j|\boldsymbol{\rho}-\boldsymbol{\rho}'|)$, and the normal derivative of the Green's function is $\partial_{n'}G_j(\boldsymbol{\rho},\boldsymbol{\rho}') \equiv (\partial/\partial n')G_j(\boldsymbol{\rho},\boldsymbol{\rho}')$. If the incident field is transverse magnetic (TM), then (1) is the electric field integral equations (EFIE); if the incident field is transverse electric (TE) then (1) is the magnetic field integral equations (MFIE). The definitions of the symbols in (1) are given in Table I for both cases where J and K denote the electric and magnetic current densities, respectively.

TABLE I
Substitution Symbols for 2-D Integral Equations

Symbol	TM	TE
F_z^{inc}	E_z^{inc}	H_z^{inc}
ϑ_j	$i\omega\mu_j$	$i\omega\varepsilon_j$
B^n	J	K
B^t	K	$-J$

If the scatterer C is partitioned into P nonoverlapping elements, the MoM system for (1) is given as [2, Ch. 4]

$$\frac{V_{qn}}{\kappa_0} = \sum_{p=1}^{P}\sum_m \frac{1}{4i\kappa_0^2}\left[\vartheta_0 Z^0_{qn,pm}\mathcal{A}_{pm} + \left\{2i\Phi^0_{qn,pm} - \zeta^0_{qn,pm}\right\}\kappa_0\mathcal{B}_{pm}\right] \tag{2a}$$

$$0 = \sum_{p=1}^{P}\sum_m \frac{1}{4i\kappa_1^2}\left[\vartheta_1 Z^1_{qn,pm}\mathcal{A}_{pm} - \left\{2i\Phi^1_{qn,pm} + \zeta^1_{qn,pm}\right\}\kappa_1\mathcal{B}_{pm}\right] \tag{2b}$$

where the currents are expanded in terms of the shape functions $S_{pm}(\boldsymbol{\rho}'_p)$, which are zero everywhere except on the pth element.

$$B_p^n(\boldsymbol{\rho}') = \sum_m \mathcal{A}_{pm}S_{pm}\left(\boldsymbol{\rho}'_p\right) \tag{3a}$$

$$B_p^t(\boldsymbol{\rho}') = \sum_m \mathcal{B}_{pm}S_{pm}\left(\boldsymbol{\rho}'_p\right). \tag{3b}$$

Likewise, the weight functions $W_{qn}(\boldsymbol{\rho}_q)$ are zero everywhere except on the qth element. The excitation terms, due to the incident field, are given by

$$V_{qn} \equiv \kappa_0 \int_{C_q} W_{qn}(\boldsymbol{\rho}_q)F_z^{\rm inc}(\boldsymbol{\rho}_q)dC_q \tag{4}$$

and the self-element symmetric-product terms are given by

$$\Phi^j_{qn,pm} \equiv \delta_{p,q}\kappa_j \int_{C_q} W_{qn}(\boldsymbol{\rho}_q)S_{qm}(\boldsymbol{\rho}_q)dC_q. \tag{5}$$

The impedance associated with the normal derivative of the field is given by

$$Z^j_{qn,pm} \equiv \kappa_j^2 \int_{C_q}\int_{C_p} H_0^{(1)}\left(\kappa_j\left|\boldsymbol{\rho}_q - \boldsymbol{\rho}'_p\right|\right) \times W_{qn}(\boldsymbol{\rho}_q)S_{pm}\left(\boldsymbol{\rho}'_p\right)dC'_p dC_q \tag{6}$$

and the impedance associated with the tangential component of the field is given by

$$\zeta^j_{qn,pm} \equiv \kappa_j \int_{C_q}\int_{C_p} \frac{\partial}{\partial n_p}H_0^{(1)}\left(\kappa_j\left|\boldsymbol{\rho}_q - \boldsymbol{\rho}'_p\right|\right) \times W_{qn}(\boldsymbol{\rho}_q)S_{pm}\left(\boldsymbol{\rho}'_p\right)dC'_p dC_q. \tag{7}$$

The calculation of the impedance terms, which are double integrals, represent a computationally complex portion of the MoM problem.

Manuscript received March 18, 2004; revised June 12, 2004. This work was supported by the Naval Surface Warfare Center, Carderock Division Intra-Laboratory Independent Research (NSWCCD-ILIR) Board under Contract 03C7S00145.

J. R. Smith, Jr. is with the Naval Surface Warfare Center, Carderock Division (NSWCCD), W. Bethesda, MD 20817-5700 USA (e-mail: smithjr@nswccd.navy.mil).

M. S. Mirotznik is with the Naval Surface Warfare Center, Carderock Division (NSWCCD), W. Bethesda, MD 20817-5700 USA and also with the Electrical Engineering Department, The Catholic University of America, Washington, DC 20064 USA (e-mail: mirotznik@cua.edu).

Digital Object Identifier 10.1109/TAP.2004.838749

[1]Note that the sign convention of $\hat{\mathbf{n}}'$ differs from [2].

[2]The presented form uses $H_0^{(1)}(\kappa|\boldsymbol{\rho}-\boldsymbol{\rho}'|)$ in the Green's function which is due to the authors' preference in sign convention.

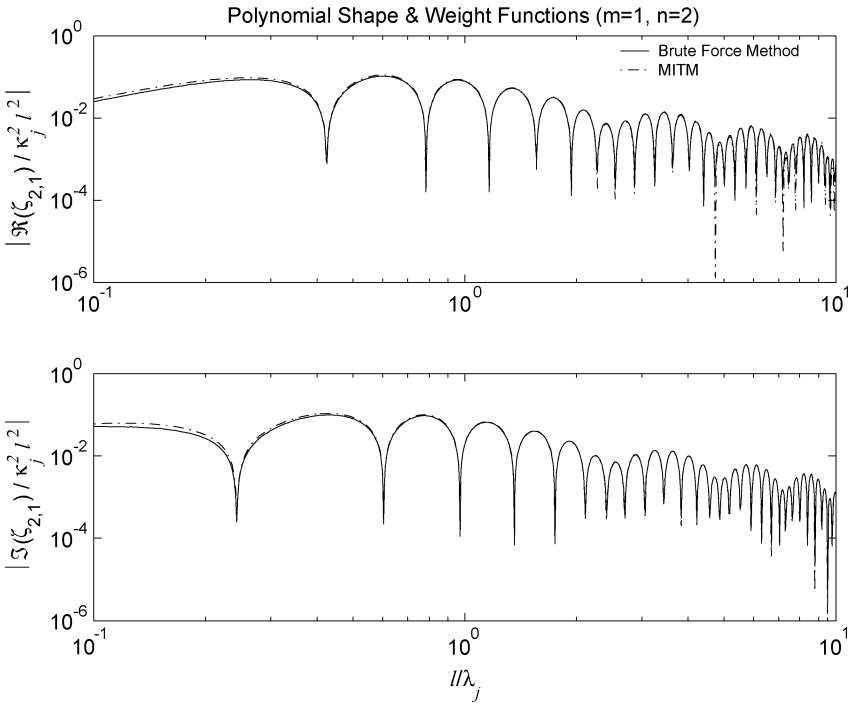

Fig. 1. Evaluation of impedance $\zeta^j_{qn,pm}$ with polynomial shape and weight functions ($m = 1$ and $n = 2$) and the geometry in Table II. The solid line is the calculation of (7) and the dashed line is the calculation of (18) and (19).

If we assume that the body C is partitioned into linear elements, then the coordinate of any position $s_p \in [0,1]$ on the pth linear element, which is L_p long, is given by

$$\boldsymbol{\rho}_p(s_p) = \boldsymbol{\rho}_p^0 + s_p L_p \hat{\mathbf{l}}_p \tag{8}$$

where $\hat{\mathbf{l}}_p$ is the unit vector along the pth element from the starting node at $\boldsymbol{\rho}_p^0 = x_p^0 \hat{\mathbf{e}}_x + y_p^0 \hat{\mathbf{e}}_y$ to the ending node point at $\boldsymbol{\rho}_p^0 + L_p \hat{\mathbf{l}}_p$. The normalized distance between any two points $\Delta^j_{p,q}(s_p, s_q) = \kappa_j |\boldsymbol{\rho}_q(s_q) - \boldsymbol{\rho}'_p(s_p)|$ is given by (9) shown at the bottom of the page, where the constant σ_p^x is the projection of $\hat{\mathbf{l}}_p$ onto the x axis ($\sigma_p^x = \hat{\mathbf{e}}_x \bullet \hat{\mathbf{l}}_p$) and similarly for σ_p^y. Defining the linear functions $\Lambda_{1,j}(s_p, s_q) \equiv A_{p,j} s_p + B_{q,j} s_q + C_{pq,j}$ and $\Lambda_{2,j}(s_p, s_q) \equiv D_{p,j} s_p + E_{q,j} s_q + F_{pq,j}$, which are related to the nondimensional horizontal distances $\kappa_j \Delta x(s_p, s_q)$ and vertical distances $\kappa_j \Delta y(s_p, s_q)$ between the test and weight sample points, yields the Green's function

$$G_j(\boldsymbol{\rho}, \boldsymbol{\rho}') \equiv \frac{1}{4i} H_0^{(1)} \left(\sqrt{\Lambda^2_{1,j}(s_p, s_q) + \Lambda^2_{2,j}(s_p, s_q)} \right). \tag{10}$$

The following section will develop an analytical method to transform (7) into a single integral.

III. Integral Substitutions for Green's 2-D Function

Smith and Mirotznik [1][3] showed that the 2-D Green's function can be expressed as the integral

$$H_0^{(1)} \left(\sqrt{\Lambda^2_{1,j} + \Lambda^2_{2,j}} \right) = \frac{2}{i\pi} \int_{\Omega^*} \frac{e^{-|\Lambda_{1,j}| u} \cos\left(\Lambda_{2,j} U(u)\right)}{U(u)} du \tag{11}$$

where the contour Ω^* goes from $-i$ to 0 to $+\infty$ and $U(u) \equiv \sqrt{u^2 + 1}$. The unit normal vector for the pth element is defined as $\hat{\mathbf{n}}_p \equiv \hat{\mathbf{e}}_z \times \hat{\mathbf{l}}_p$. Using the relationship $\partial/\partial n_p = \hat{\mathbf{n}}_p \cdot \boldsymbol{\nabla} = \sigma_p^x (\partial/\partial y) - \sigma_p^y (\partial/\partial x) =$ $\sigma_p^x \kappa_j (\partial/\partial \Lambda_{2,j}) - \sigma_p^y \kappa_j (\partial/\partial \Lambda_{1,j})$, we see that the derivative of (11) with respect to the normal of the sample element p is then given by

$$\frac{\partial H_0^{(1)}\left(\Delta^j_{p,q}(s_p, s_q)\right)}{\partial n_p} = \sigma_p^y \frac{2\kappa_j}{i\pi} \int_{\Omega^*} u \frac{e^{-\Lambda_{1,j} u} \cos\left[\Lambda_{2,j} U(u)\right]}{U(u)} du - \sigma_p^x \frac{2\kappa_j}{i\pi} \int_{\Omega^*} e^{-\Lambda_{1,j} u} \sin\left[\Lambda_{2,j} U(u)\right] du \tag{12}$$

where $\Lambda_{1,j}(s_p, s_q) > 0$ is required by (11). Substituting (12) into (7) and separating the result into two integrals as

$$\zeta^j_{qn,pm} = \sigma_p^y \zeta^{j,(1)}_{qn,pm} - \sigma_p^x \zeta^{j,(2)}_{qn,pm} \tag{13}$$

where the first term $\zeta^{j,(1)}_{qn,pm}$ contains the first integral of (12) and the second term $\zeta^{j,(2)}_{qn,pm}$ contains the second integral in (12), yields the triple integral expressions

$$\begin{aligned} \zeta^{j,(\beta)}_{qn,pm} \equiv \frac{L_p L_q \kappa_j^2}{i\pi} & \int_{\Omega^*} e^{-C_{pq,j} u} T_\beta(u) du \\ & \times \int_{s_p=0}^{s_p=1} e^{-A_{p,j} s_p u} S_{pm}(s_p) ds_p \\ & \times \int_{s_q=0}^{s_q=1} e^{-B_{q,j} s_q u} W_{qn}(s_q) ds_q \\ & \times \begin{bmatrix} e^{iD_{p,j} s_p U(u)} e^{iE_{q,j} s_q U(u)} e^{iF_{pq,j} U(u)} \\ \pm e^{-iD_{p,j} s_p U(u)} e^{-iE_{q,j} s_q U(u)} e^{-iF_{pq,j} U(u)} \end{bmatrix} \end{aligned} \tag{14}$$

TABLE II
Coordinates of Element Nodes

Element p	Element q
$(0,0)$ to $(l,0)$	(l,l) to $(l,2l)$

[3]In the present form, u and Ω^* have been normalized by κ_j.

$$\Delta^j_{p,q}(s_p, s_q) = \sqrt{\kappa_j^2 \left(x_p^0 + s_p L_p \sigma_p^x - x_q^0 - s_q L_q \sigma_q^x\right)^2 + \kappa_j^2 \left(y_p^0 + s_p L_p \sigma_p^y - y_q^0 - s_q L_q \sigma_q^y\right)^2} \tag{9}$$

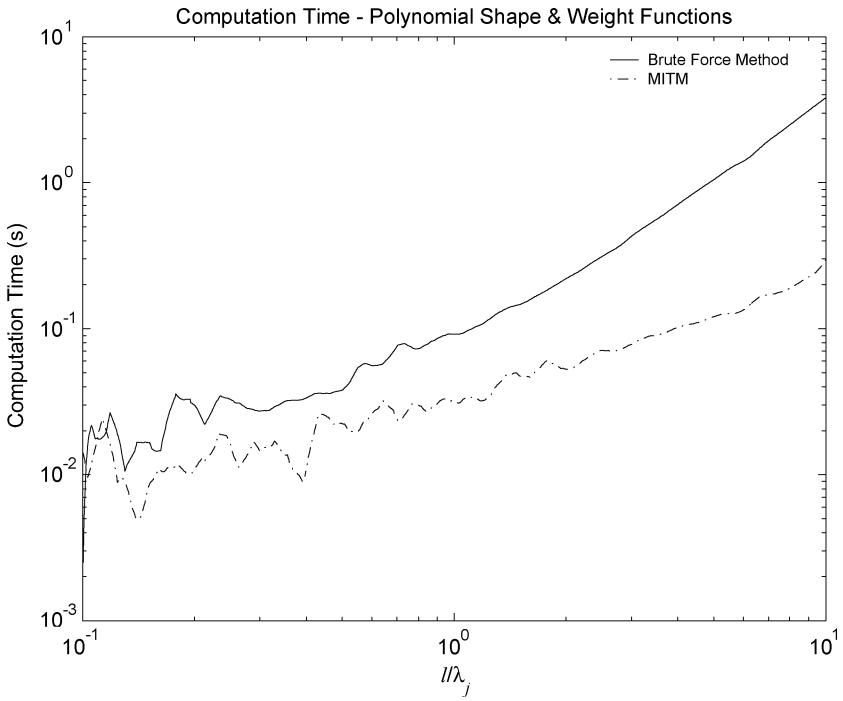

Fig. 2. Computation times for the brute force method and MITM calculations of $\zeta^{j}_{qn,pm}$. Calculations were performed using MatLab R13 on a 1.4 GHz PentiumIV with 1 Gb of RAM. The brute force method computation time is quadratic in l/λ_j while the MITM computation time is linear in l/λ_j.

where $T_1(u) = u/U(u)$ and $T_2(u) = -i$. The positive sign in (14) is selected for $\beta = 1$ and negative sign for $\beta = 2$. For the distinct element cases ($p \neq q$), (14) can be expressed in terms of the functions

$$\mathbb{I}^{j,(1)}_{qn,pm}[u] \equiv \mathbb{S}_{pm}[u; A_{p,j}, D_{p,j}]\mathbb{W}_{qn}[u; B_{q,j}, E_{q,j}] \times \exp\left[-C_{pq,j}u - iF_{pq,j}U(u)\right] \tag{15}$$

$$\mathbb{I}^{j,(2)}_{qn,pm}[u] \equiv \mathbb{S}_{pm}[u; A_{p,j}, -D_{p,j}]\mathbb{W}_{qn}[u; B_{q,j}, -E_{q,j}] \times \exp\left[-C_{pq,j}u + iF_{pq,j}U(u)\right] \tag{16}$$

where $\mathbb{S}$ and $\mathbb{W}$ are the transformed shape and weight functions [1], respectively. The transform of the shape function S is $\mathbb{S}$, given by

$$\mathbb{S}[u; \alpha, \beta] = \int_{s=0}^{s=1} S(s)e^{-\alpha s u - i\beta s\sqrt{u^2+1}}ds \tag{17}$$

similarly for W and $\mathbb{W}$. This is the transformation performed in [1] and is denoted as the $\mathcal{R}$ transformation.

Using (15) and (16), the impedance terms $\zeta^{j,(1)}_{qn,pm}$ and $\zeta^{j,(2)}_{qn,pm}$ simplify to the single integral expressions

$$\zeta^{j,(1)}_{qn,pm} = \frac{L_p L_q \kappa_j^2}{\pi i}\int_{\Omega^*} u\,\frac{\mathbb{I}^{j,(1)}_{qn,pm}[u] + \mathbb{I}^{j,(2)}_{qn,pm}[u]}{\sqrt{u^2+1}}du \tag{18}$$

$$\zeta^{j,(2)}_{qn,pm} = \frac{L_p L_q \kappa_j^2}{\pi}\int_{\Omega^*} \left\{\mathbb{I}^{j,(1)}_{qn,pm}[u] - \mathbb{I}^{j,(2)}_{qn,pm}[u]\right\}du \tag{19}$$

and, from [1],[4] the impedance term $Z^{j}_{qn,pm}$ simplifies to

$$Z^{j}_{qn,pm} = \frac{L_p L_q \kappa_j^2}{\pi i}\int_{\Omega^*} \frac{\mathbb{I}^{j,(1)}_{qn,pm}[u] + \mathbb{I}^{j,(2)}_{qn,pm}[u]}{\sqrt{u^2+1}}du. \tag{20}$$

Therefore, all the impedance terms in (2a) and (2b) can be reduced to single integral expressions using (18)–(20) whenever $p \neq q$. This generalizes the MITM for distinct elements cases.[5]

[4]The coeffient in [1] differs from the present form. The form in (20) is consistent with (6). Also, u and Ω^* are normalized by κ_j.

[5]For linear elements, $\zeta^{j}_{qn,pm}$ is zero when $p = q$ (self-element). See [1] for the $Z^{j}_{qn,pm}$ self-element MITM expression.

It should be noted that for certain geometric configurations, $\zeta^{j,(1)}_{qn,pm}$ can be less stable than $\zeta^{j,(2)}_{qn,pm}$. However, since only the relative geometric configurations of two elements are important to the impedance, a coordinate rotation can be performed on an element pair so that $\sigma^y_p = 0$ and $\sigma^x_p = 1$ thereby eliminating (18). Any coordinate rotation must also ensure that $\Lambda_1 > 0$ remains true. For adjacent elements, $\Lambda_1 = 0$ at the shared node. To handle this case, perturb the the shared node on one element so that Λ_1 remains positive.

IV. Evaluation of $\zeta^{j}_{qn,pm}$ for Polynomials

If $S_{pm}(s_p) = s_p^m$, then its $\mathcal{R}$ transformation ($\mathbb{S}_{pm}[u] \equiv \mathbb{S}_{pm}(u; A_{p,j}, \pm D_{p,j})$) is given by [1]

$$\mathbb{S}_{p0}[u] = \frac{1 - e^{-r}}{r} \text{ for } m = 0 \tag{21}$$

$$\mathbb{S}_{pm}[u] = \frac{m\mathbb{S}_{p(m-1)}[u] - e^{-r}}{r} \text{ for } m > 0 \tag{22}$$

where $r(u) = A_{p,j}\,u \pm iD_{p,j}\sqrt{u^2+1}$.

Fig. 1, presents a numerical comparison between the brute force calculation of the general impedance (7) and the MITM integrals (18) and (19) for the geometry described in Table II where l is an arbitrary length. The shape and weight functions are polynomials with $m = 1$ and $n = 2$. The brute force evaluations of (7) employed a Simpson's Rule integration scheme with $\lambda_j/40$ sampling. The evaluations of (18) and (19) also used a Simpson's Rule with approximately $5000\,l/\lambda_j$ samples for the finite path and $500\,l/\lambda_j$ samples for the infinite path. Although Ω^* is infinite, the integrands approach 0 exponentially allowing the integrations to be truncated[6] before $u = 20\,l/\lambda_j$. The singularity in (18) at $u = -i$ was avoided by adding $\epsilon = 10^{-4}$ to the singular point.

It is clear from Fig. 1 that the brute force method and MITM evaluations of ζ produce nearly identical results. Fig. 2 compares the computation times of the two methods. As the size of the element increases, the time savings of using the MITM technique increases significantly with over an order of magnitude reduction for the largest case presented.

[6]At $u = 20\,l/\lambda_j$, the integrand is generally less than 10^{-10}.

V. Conclusion

The MoM impedance equations for the general EFIE and MFIE can be simplified to single integrals for a wide range of shape and weight functions. The resulting MITM expressions in (18)–(20) reduce the computational complexity of evaluating the impedances.

Acknowledgment

The authors wish to thank the Naval Surface Warfare Center, Carderock Division ILIR program for funding this work. Additionally, the authors are indebted to the reviewers for significantly improving this communication.

References

[1] J. R. Smith Jr. and M. S. Mirotznik, "Analytical simplification of the 2-D method of moments impedance integral," *IEEE Trans. Antennas Propat.*, vol. 52, no. 12, pp. 3288–3294, Dec. 2004.

[2] N. Morita, N. Kumagai, and J. R. Mautz, *Integral Equation Methods for Electromagnetics*. Boston, MA: Artech House, 1990, p. 18, 149-163, 236-288.

Variation in Bandwidths Among Solutions to Shaped Beam Synthesis Problems Concerning Linear Arrays of Parallel Dipoles

J. C. Brégains and F. Ares

***Abstract*—The problem of synthesizing a linear array generating a shaped beam pattern with M filled nulls has 2^M alternative solutions. In this study we examined their bandwidths as regards compliance with pattern quality or input impedance requirements in the presence and absence of a backing ground plane. Placing a ground plane behind the antenna almost doubles sidelobe level bandwidth.**

***Index Terms*—Bandwidth, equispaced linear arrays, shaped beam patterns.**

I. Introduction

As is well known, the filled nulls of a shaped beam pattern generated by a linear array of N radiating elements spaced a distance d apart correspond to those roots of the equation

$$\sum_{n=1}^{N} I_n w^{n-1} = 0 \tag{1}$$

that lie off the Schelkunoff unit circle, where I_n is the excitation of the nth element and $w = \exp[j(2\pi d/\lambda)\cos\theta]$, with θ measured from endfire. It has often been pointed out [1], [2] that any such off-circle root, $\exp(a_n + jb_n)$ say, can be replaced by $\exp(-a_n + jb_n)$ without altering the radiation power pattern. As a result, there are in general 2^M solutions for a pattern with M filled nulls, although the number of independent solutions will be smaller if symmetry constraints are introduced [2]. This multiplicity of solutions has in the past been taken advantage of by choosing from among their number the solution consisting of what appeared to be the excitation distribution least likely to be affected by problems due to mutual coupling among the elements, which in the case of dipole arrays has usually been identified as the one with the smallest value of $|I|_{\max}/|I|_{\min}$ or $(|I_n|/|I_n \pm_1|)_{\max}$, where $|I|_{\max}$ and $|I|_{\min}$ are respectively the largest and smallest of the $|I_n|$.

In this Communication, we investigated whether there can be solutions with significant advantages as regards bandwidth with respect to pattern quality or embedded impedance; compared the bandwidths of the 2^M solutions described above with those of a system consisting of a symmetric pure real excitation distribution generating a flat-topped beam of approximately equal width as in the above cases (for this it is necessary to introduce extra array elements [2]); and investigated the influence of a nearby ground plane on these findings. In all these calculations we considered an array of parallel dipoles spaced $\lambda/2$ apart.

II. Method

A. General Solutions in the Absence of a Ground Plane

We considered an array of 20 parallel dipoles of length $\lambda_D/2$ and radius 0.004 763 λ_D, all parallel to the x axis and spaced $\lambda_D/2$ apart along the z axis, where λ_D is the design frequency. For this array we used the Orchard–Elliott method [1] to find a solution to the problem of synthesizing a symmetric flat-topped shaped beam pattern with $M = 6$ filled nulls, a beamwidth of about 52° between nulls, ± 0.5 dB of ripple, and a maximum sidelobe level of -20 dB (Fig. 1, continuous curve). This method directly affords the roots $\exp(a_n + jb_n)$ of (1), and we then found the other 63 excitation distributions giving the same radiation power pattern by generating all possible combinations of signs of the six nonzero a_n.

For each of the distributions $\{I_n\}$ so obtained, we next obtained the required input voltages V_n from the expression

$$V_n = \sum_{m=1}^{N} Z_{nm} I_m \tag{2}$$

where the Z_{nm} are the self and mutual impedances of the elements, which were calculated as per Hansen [3]; and we then obtained the embedded impedances (or active impedances) $Z_n^e = V_n/I_n$. Finally, we investigated the tolerance of the solutions to deviations from the design frequency f_D as regards the embedded impedance characteristics $|Z_1^e|$, $|R_1^e|$, $|X_1^e|$, $|Z_{10}^e|$, $|R_{10}^e|$, $|X_{10}^e|$, $|Z^e|_{\max}$, $|R^e|_{\max}$, and $|X^e|_{\max}$ (where $Z_n^e = R_n^e + jX_n^e$) and the ripple, sidelobe level and -3 dB beamwidth of the corresponding power patterns in the yz plane ($\varphi = 90°$). The impedances of the central element (10) and the edge element (1) were chosen for special attention because, like the present array, most shaped beam arrays have enough elements for the design to be based on these impedances. For each solution we fixed the V_n obtained above (arrays generating shaped beams are almost always designed on a constant voltage basis) and for each of a sequence of frequencies differing by $\Delta f = f_D/300$ we calculated first the corresponding Z_{nm} (as per Hansen [3]) and then the corresponding I_m [by solving (2)] and the resulting power patterns (for which the array factor given by the I_n was multiplied by the element factor). By this means we determined $f_U = f_U^* - \Delta f$ and $f_L = f_L^* + \Delta f$ (where f_U^* and f_L^* are, respectively, the lowest frequency higher than f_D and the highest frequency lower than f_D at which the test characteristic differed by more

Manuscript received March 29, 2004. This work was supported by the Spanish Ministry of Science and Technology under project TIC 2002-04084-C03-02.

The authors are with the Grupo de Sistemas Radiantes, Departamento de Física Aplicada, Facultad de Física, Universidad de Santiago de Compostela, 15782 Santiago de Compostela, Spain (e-mail: faares@usc.es).

Digital Object Identifier 10.1109/TAP.2004.836394